ELSEVIER

Catalysis Today 57 (2000) 177–186

CATALYSIS TODAY

www.elsevier.com/locate/cattod

Modification of vanadium phosphorus oxides used for *n*-butane oxidation to maleic anhydride by interaction with niobium phosphate

P.G. Pries de Oliveira [a,*], J.G. Eon [b], M. Chavant [c], A.S. Riché [c], V. Martin [c], S. Caldarelli [c], J.C. Volta [c]

[a] *Instituto Nacional de Tecnologia, Avenida Venezuela 82, Praça Maua 20081, Rio de Janeiro, Brazil*
[b] *Instituto de Quimica, Universidade Federal do Rio de Janeiro, Cidade Universitaria, Ilha do Fundao 21945-970, Rio de Janeiro, Brazil*
[c] *Institut de Recherches sur la Catalyse, 2 Avenue A. Einstein 69626, Villeurbanne Cédex, France*

Abstract

A new family of vanadium phosphorus oxides (VPO) catalysts has been identified. It consists in a mixture of VPO with niobium phosphate (NbPO). The amorphous NbPO material is introduced during the preparation of the $VOHPO_4{\cdot}0.5H_2O$ precursor. It is observed that the VPO–NbPO catalyst is more rapidly activated and gives better performances (*n*-butane conversion and maleic anhydride selectivity) for mild oxidation of *n*-butane to maleic anhydride. VPO phases and the NbPO material have been identified in the VPO–NbPO precursor and in the VPO–NbPO catalyst. Nb in VPO crystals and V in NbPO particles have been respectively observed by EDX-STEM. No other VPO crystals than the $VOHPO_4$, $0.5H_2O$ precursor, and $(VO)_2P_2O_7$ for the catalyst, have been identified by XRD and ^{31}P NMR. ^{31}P NMR by spin echo mapping and ^{31}P MAS NMR have confirmed an interaction of the VPO precursor with Nb and of the NbPO amorphous material with V, as evidenced by EDX-STEM. This should be the reason for the observed improvement of the catalytic results by a redox effect of niobium on the VPO catalyst modifying the V^{5+}/V^{4+} balance in a favourable way.

Keywords: Vanadium phosphorus oxide; Oxidation; Niobium phosphate

1. Introduction

Vanadium phosphorus oxides (VPO) is a well known family of catalysts for the mild oxidation of *n*-butane to maleic anhydride [1–3]. The effective VPO catalyst needs a long activation of the $VOHPO_4$, $0.5H_2O$ precursor (V^{4+}) which changes into $(VO)_2P_2O_7$ (V^{4+}) under the *n*-C_4/air flow, with a suitable dispersion of isolated V^{5+} sites in strong interaction with $(VO)_2P_2O_7$, depending on the catalytic conditions [4–6]. Industrially, the activation of the VPO catalysts to the "equilibrated catalysts" needs more than 1000 h in a classical fixed bed reactor. In order to diminish the costs in industrial units, it is highly important to decrease the activation time. In parallel, the need to improve the catalytic performances of the VPO catalyst has prompted research on the corresponding materials by introducing dopants [7], or by attempting to support the VPO catalyst [8–10]. In this communication, we show, in agreement with previous work [10,11], that niobium phosphate (NbPO) is a good material to improve both the catalytic performances for *n*-butane oxidation to maleic anhydride, and to decrease the time of activation of the VPO catalyst. The effect of NbPO on the properties of the VPO precursors and catalysts is discussed.

* Corresponding author.

0920-5861/00/$ – see front matter
PII: S0920-5861(99)00324-7

2. Experimental

2.1. Preparation of the VPO–NbPO precursors

The niobium phosphate (NbPO) was obtained from the Companhia Brasileira de Metalurgia e Mineraçao (CBMM). It is a poorly crystallised material with a BET area of 180 m^2/g. The VPO–NbPO precursors were prepared following the classical Exxon method by refluxing V_2O_5 with isobutanol and H_3PO_4 (85%) for the preparation of $VOHPO_4$, $0.5H_2O$ [12]. The VPO–NbPO precursors which gave the best VPO–NbPO catalysts had to be prepared by introducing NbPO just before the nucleation of the $VOHPO_4$, $0.5H_2O$ vanadyl phosphohemihydrate in the organic medium. For example 3.20 g of V_2O_5 (RdH) was refluxed with 100 ml isobutanol (Merck) and 4.48 g H_3PO_4 85% for 35 min. After cooling to room temperature, the white powder of the NbPO material was then introduced in the mixture which was further refluxed for 24 h. The blue final precipitate was then centrifuged at room temperature, washed with isobutanol and ethanol and dried at 110°C for 16 h. We prepared different precursors by changing the mass of NbPO as compared with V_2O_5 initially introduced in the preparation. The precursors and catalysts will be indexed as $VPO_{(3.2)}$–$NbPO_{(X)}$ (where 3.2 g is the mass of V_2O_5 initially used and X g the mass of NbPO further introduced). Two precursors and catalysts will be particularly considered in this work: $VPO_{(3.2)}$–$NbPO_{(0.5)}$ and $VPO_{(3.2)}$–$NbPO_{(1)}$.

2.2. Activation of the VPO–NbPO precursors

The VPO–NbPO precursors were activated in the catalytic reactor under *n*-butane/air atmosphere in the following conditions: *n*-C_4/O_2/He=1.6/18/80.4 −GHSV=1500 h^{-1}. Performances (*n*-C_4 conversion and MA selectivity) were measured after a period of 120 h of activation which are normally necessary in the laboratory conditions for a massic VPO catalyst to be equilibrated.

2.3. Physicochemical characterisation

Precursors and catalysts were characterised by XRD using a Siemens diffractometer and Cu Kα radiation. A Scanning Electron Microscope Hitachi S 800 was used to study the morphology of the materials. An EDX-STEM Microscope JEOL JSM-840/A allowed the analysis of V, Nb and P depending on the different morphologies observed by SEM. These results were compared with the chemical analysis of the materials. TGA experiments of the transformation of the precursors under air (ΔT=5°C/min) were performed in a SETARAM TGA-92/12 microbalance with a simultaneous registration of the heat flow (HF). ^{31}P NMR experiments were performed on a BRUKER MSL 300 NMR spectrometer. Conventional spectra were obtained at 121.5 MHz using a 90°x-(acquire) sequence. The 90° pulse was 4.2 μs and the delay time between two consecutive scans was 10 s. Samples were typically spun at 4 kHz in zirconia rotors using a double bearing probehead. The ^{31}P Spin Echo spectra were recorded under static conditions, using a 90°x-τ–180°y-τ- (acquire sequence). The 90° pulse was 4.2 μs and τ was 20 μs. For each sample, the irradiation frequency was varied in increments of 100 kHz above and below the ^{31}P resonance of H_3PO_4. The number of spectra thus recorded was dictated by the frequency limits beyond which no spectral intensity was visible. The ^{31}P NMR Spin Echo Mapping information was then obtained by superposition of all spectra.

Catalytic measurements for oxidation of *n*-butane to maleic anhydride were performed at 400°C and at atmospheric pressure with 400 mg of catalyst in a microreactor in the corresponding conditions: $n-C_4/O_2$/He=1.6/18/80.4−GSHV=1500 h^{-1}.

3. Results

3.1. About the precursors

The XRD spectra of the two precursors $VPO_{(3.2)}$–$NbPO_{(0.5)}$ and $VPO_{(3.2)}$–$NbPO_{(1)}$ are presented in Fig. 1. They are characteristic of the $VOHPO_4$, $0.5H_2O$ phase. No other phases are observed. Recall that the NbPO material is amorphous and cannot be detected by XRD. However the major lines are particular for both spectra with a higher contribution of the (220) line as compared to the (001) one which is, in this case, also enlarged. This is typical of the

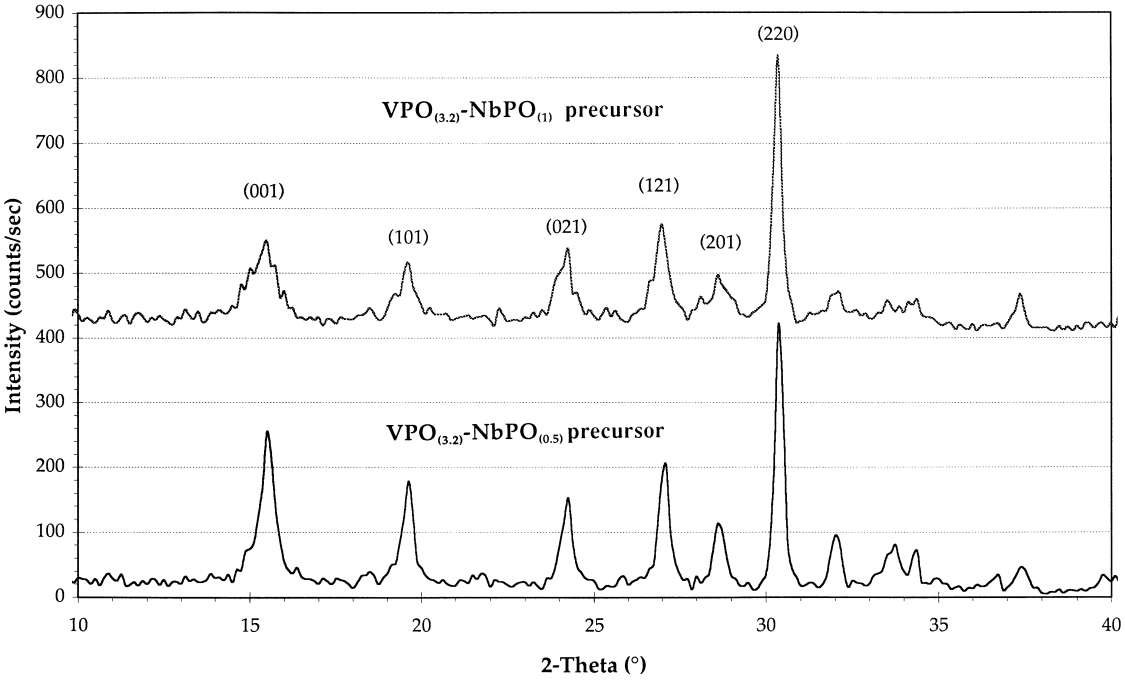

Fig. 1. XRD spectra of the VPO–NbPO precursors as refered to normal $VOHPO_4$, $0.5H_2O$.

morphology obtained by reduction of $VOPO_4{\cdot}2H_2O$ by isobutanol [12] which is known to develop VPO crystals with thin $VOHPO_4$, $0.5H_2O$ (001) platelets (VPD route). The BET area of the VPO–NbPO precursors is given in Table 1. It increases with the NbPO contribution.

Fig. 2 presents the HF spectra under air of the same precursors as compared to the reference $VOHPO_4$, $0.5H_2O$ precursor and to the reference NbPO material. As previously published [13], endothermic effects in the 340–410°C temperature range are associated with the dehydration of $VOHPO_4$, $0.5H_2O$ into $(VO)_2P_2O_7$, while the exothermic peak at 505–510°C is due to its reoxidation into $VOPO_4$ phases (see VPO reference). It clearly appears that these two transformations typical of the $VOHPO_4$, $0.5H_2O$ hemihydrate are also observed for the two VPO–NbPO precursors. Two exothermic phenomena located near 215 and 265–275 are observed on the HF spectra of the VPO–NbPO precursors. The peak at 215°C is due to the oxidation of isobutanol as it is observed from an experiment on a reference impregnated isobutanol–NbPO material. The peak at 265–275°C appears to be also a fingerprint of NbPO. The increase of the NbPO contribution in the VPO–NbPO precursors induces a decrease of the temperature of dehydration of $VOHPO_4$, $0.5H_2O$ (from 410 down to 400°C between VPO and $VPO_{(3.2)}$–$taNbPO_{(1)}$).

Table 1
BET area of the VPO–NbPO precursors as compared to the NbPO material

	NbPO material	$VPO_{(3.2)}$–$NbPO_{(1)}$	$VPO_{(3.2)}$–$NbPO_{(0.5)}$
BET area (m^2/g)	180	31.8	19.5

The ^{31}P SEM NMR spectra of the VPO–NbPO precursors are presented in Fig. 3. A signal is observed at 1728 ppm ($VPO_{(3.2)}$–$NbPO_{(0.5)}$) and at 1740 ppm ($VPO_{(3.2)}$–$NbPO_{(1)}$). It appears characteristic of P atoms in the vicinity of V atoms in $VOHPO_4$, $0.5H_2O$ (1625 ppm) [14], but displaced to higher value. A second signal is observed at −9.5, −10.5 ppm which has been attributed to P atoms in the vicinity of NbPO.

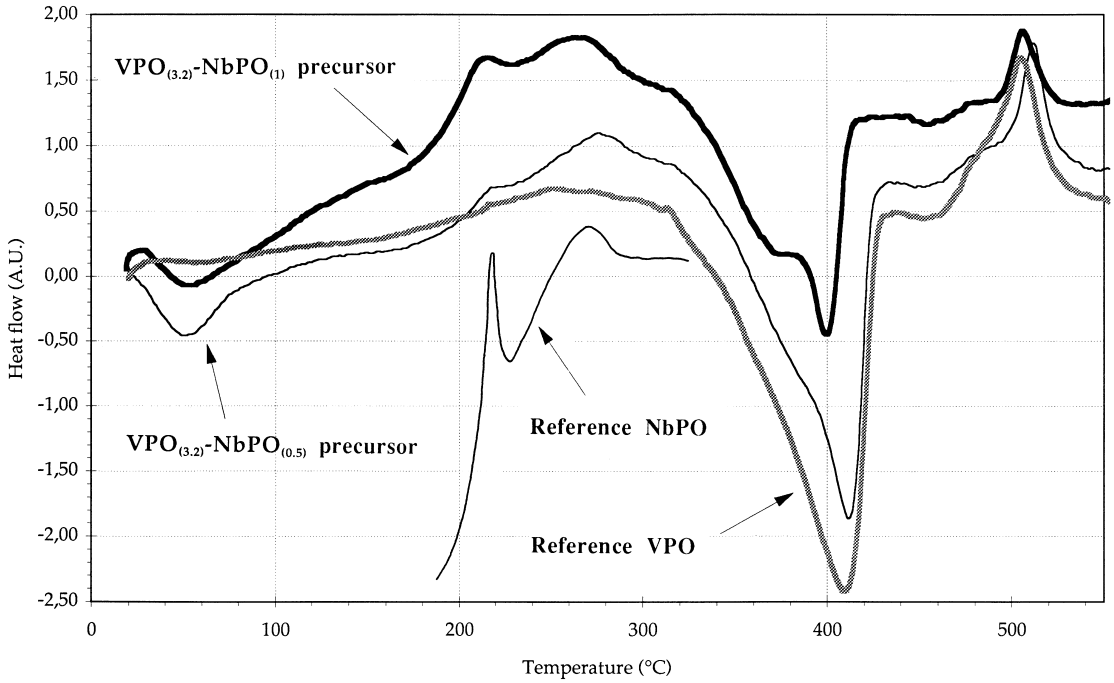

Fig. 2. Heat flow spectra of the activation under air of the VPO–NbPO precursors as refered to $VOHPO_4$, $0.5H_2O$ and to the NbPO material during TGA experiments.

The reference NbPO shows a ^{31}P MAS NMR spectrum signal at −8.0 ppm which differs from the ^{31}P MAS NMR spectrum signal of $VOHPO_4$, $0.5H_2O$ at 1.7 ppm (see Fig. 4a). ^{31}P MAS NMR spectra of the VPO–NbPO precursors are presented in Fig. 4b as a function of the Nb content in the 0.1–0.5 g range of preparation. Two signals which correspond to two different environments of P atoms are observed. The signal near −9, −10 ppm is typical of NbPO while the signal at 2.1 ppm belongs to $VOHPO_4$, $0.5H_2O$ (see Fig. 4a).

Fig. 5 shows the SEM study on the $VPO_{(3.2)}$–$NbPO_{(1)}$ precursor. Four different morphologies are observed:

N large particles typical of the NbPO material;
P entangled $VOHPO_4$, $0.5H_2O$ crystals as platelets which appear to have grown on the NbPO material.
R $VOHPO_4$, $0.5H_2O$ platelets organised as typical sand-roses.
S isolated squamas of $VOHPO_4$, $0.5H_2O$ crystals usually deposited on the NbPO material.

From this study, it appears that different morphologies of $VOHPO_4$, $0.5H_2O$ crystals are observed. This may be the influence of the interaction with NbPO.

The results of the EDX-STEM examination of the corresponding precursor is presented in Fig. 6. It compares the atomic composition depending on the different morphologies (Fig. 5). G corresponds to a general examination of the precursor which integrates all the SEM observed morphologies. It shows the corresponding composition considering V+P+Nb=100 (46.5%V, 46.1%P, 7.4%Nb). Nb/V=0.159 from this study, which approaches the result of the chemical analysis (Nb/V=0.152). It appears from Fig. 6 that some V is present on or into the N NbPO isolated crystals. The analysis of the P entangled $VOHPO_4$, $0.5H_2O$ crystals alone is difficult since they are always covering N NbPO crystals. This is the same situation for the S isolated $VOHPO_4$, $0.5H_2O$ squamas

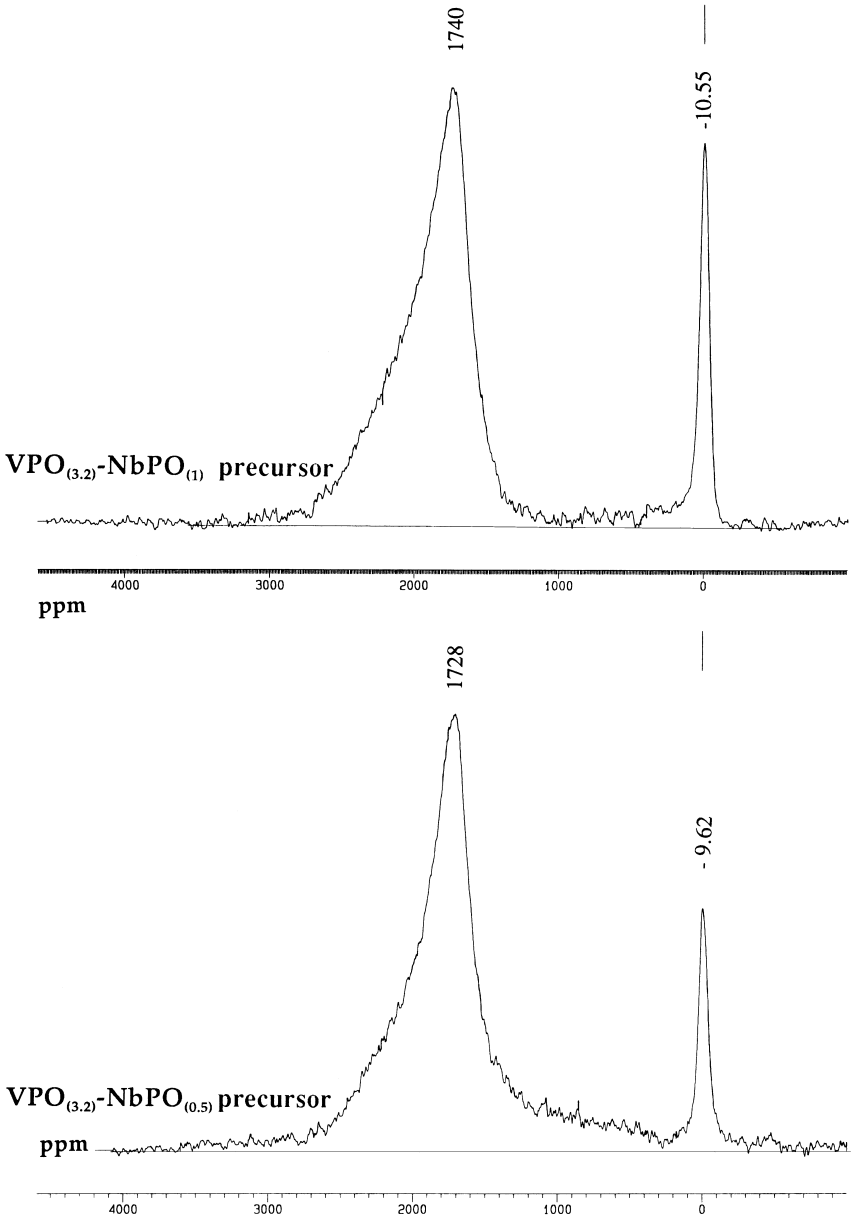

Fig. 3. ^{31}P SEM NMR spectra of the VPO–NbPO precursors.

often dispersed on N NbPO crystals. When isolated R entangled $VOHPO_4$, $0.5H_2O$ crystals or isolated S $VOHPO_4$, $0.5H_2O$ squamas are considered, some Nb is analysed together with the major V element. In that case the P/V ratio was 1.01 and 0.99, respectively which is the expected ratio of $VOHPO_4$, $0.5H_2O$. It was concluded from this study that there was some Nb on or into $VOHPO_4$, $0.5H_2O$ and some V on or into NbPO.

3.2. About the catalysts

Best catalytic results were obtained for VPO–NbPO corresponding to low Nb/V ratios. The VPO–NbPO

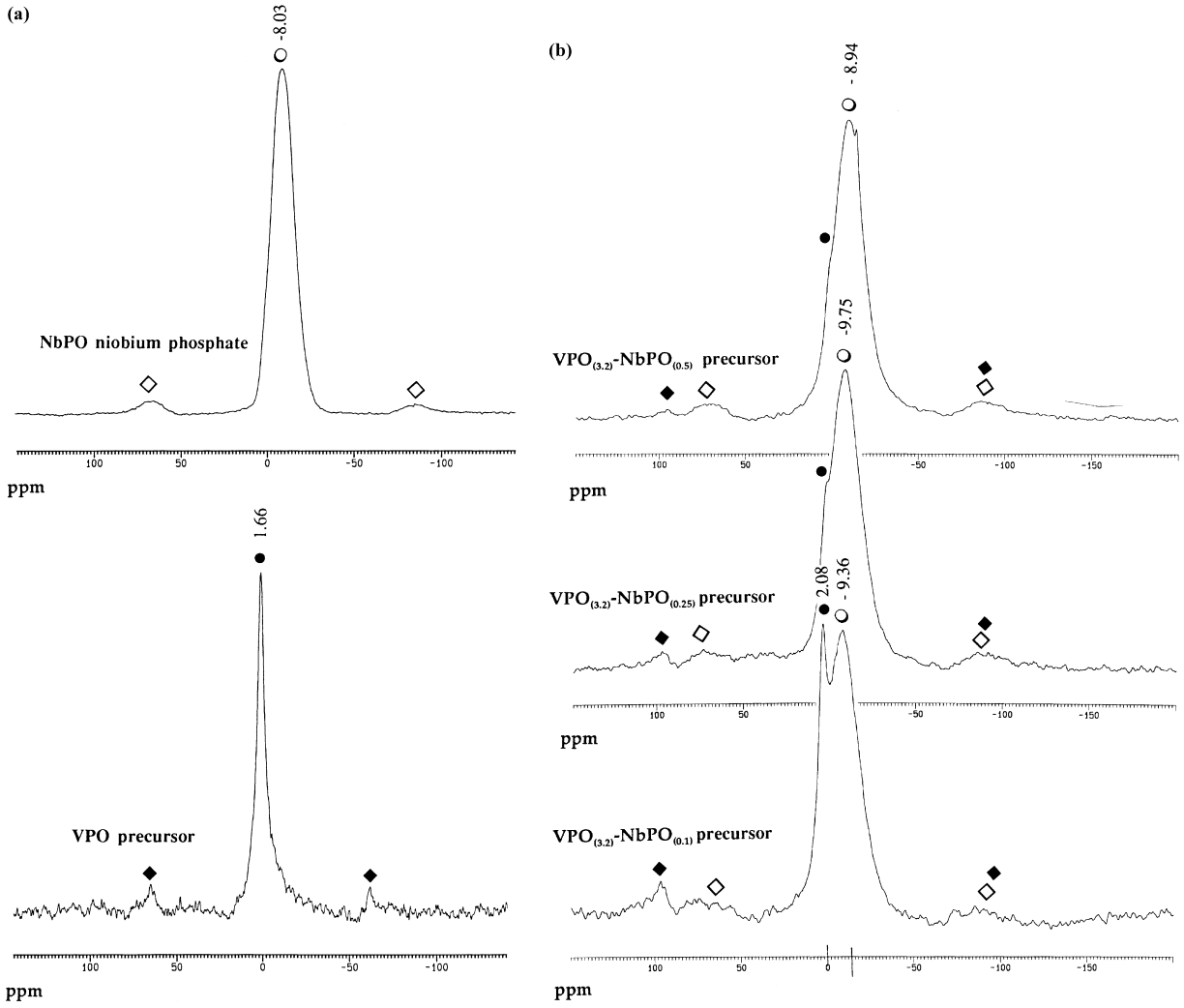

Fig. 4. (a) ^{31}P MAS NMR spectra of the reference NbPO niobium phosphate and of the VPO precursor ($VOHPO_4$, $0.5H_2O$); (b) ^{31}P MAS NMR spectra of the VPO–NbPO precursors at low NbPO content. (○) Band characteristic of the NbPO niobium phosphate; (◇) corresponding rotating bands; (●) band characteristic of the VPO precursor; (◆) corresponding rotating bands.

catalysts reach a stationary state after only 40 h, while, in the same conditions, the massic VPO catalysts need more than 120 h. The following table gives the catalytic performances measured after 40 h of activation at 400°C of the corresponding precursors ($n-C_4/O_2$/He: 1.6/18/80.4−GSHV=1500 h^{-1}) for two different VPO–NbPO compositions in comparison with the massic VPO.

Catalysts	n-C_4 conversion (%)	MA selectivity (%)	MA yield (%)
Massic VPO	40	62	24.8
$VPO_{(3.2)}$–$NbPO_{(1)}$	60	75	45.0
$VPO_{(3.2)}$-$NbPO_{(0.5)}$	75	75	54.2

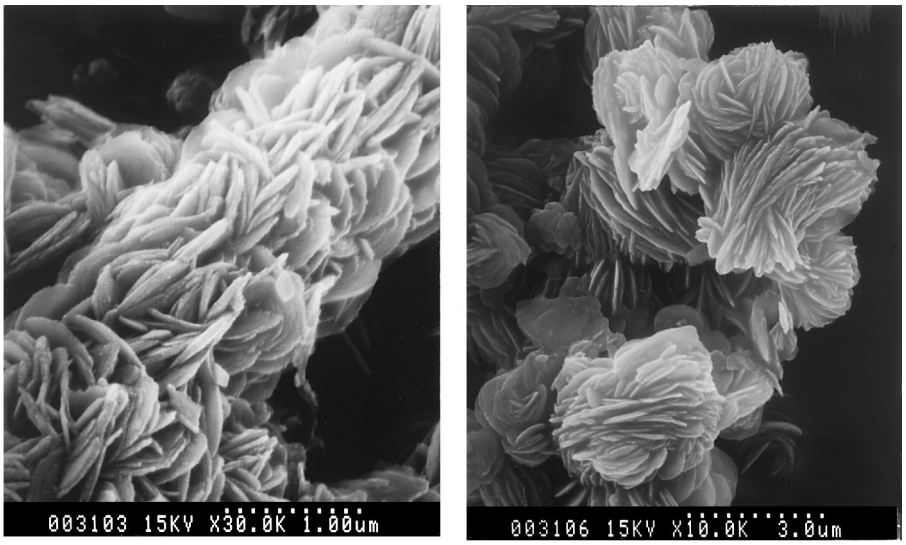

Entangled $VOHPO_4.0.5\ H_2O$ crystals (**P**) $VOHPO_4.\ 0.5\ H_2O$ sand-roses (**R**)

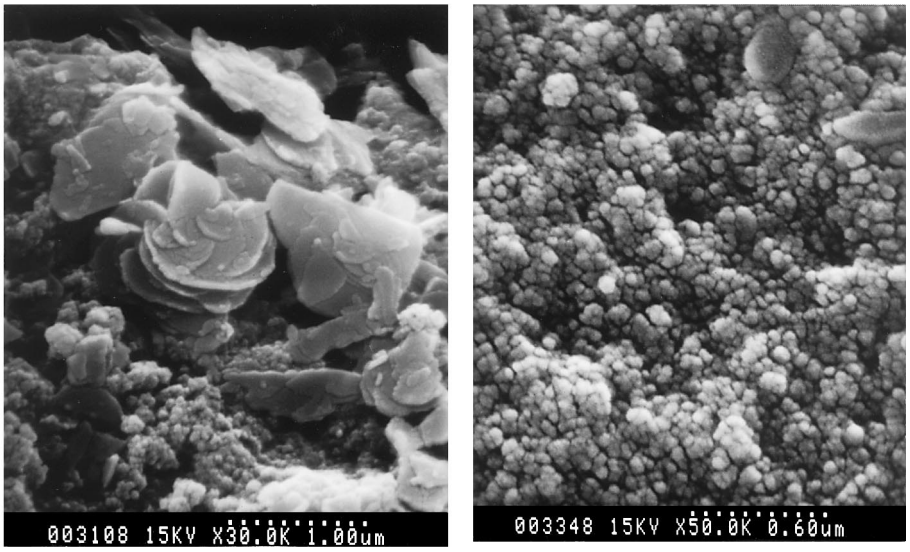

Sqasmas of $VOHPO_4.0.5\ H_2O$ crystals (**S**) deposited on NbPO (**N**)

Surface of the NbPO material (**N**)

Fig. 5. SEM examination of the $VPO_{(3.2)}$–$NbPO_{(1)}$ precursor showing the four different morphologies of VPO and NbPO.

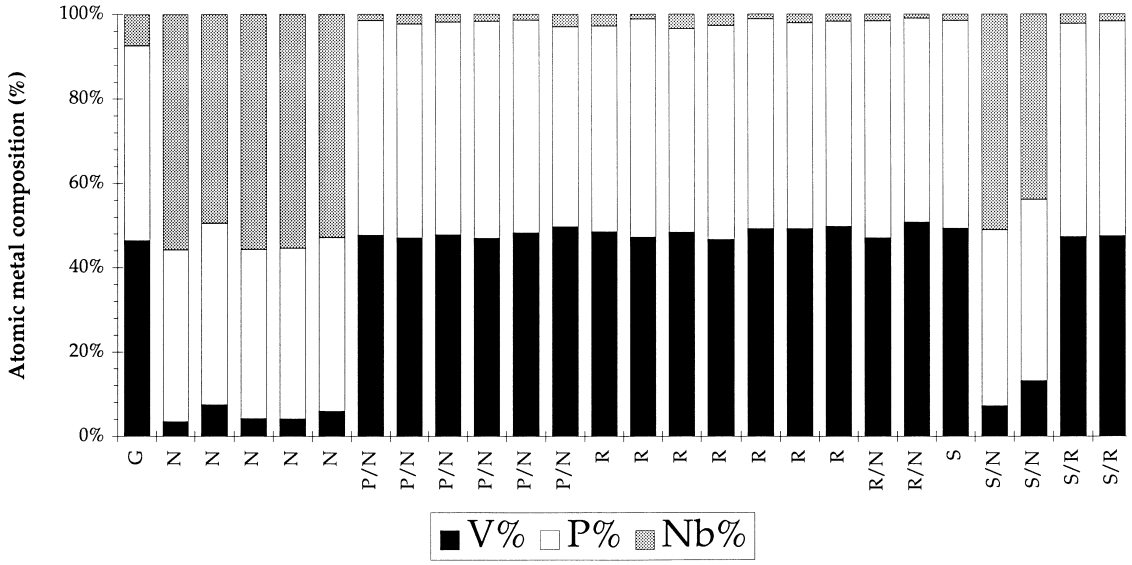

Fig. 6. EDX-STEM analysis of the four different morphologies of VPO and NbPO.

n-butane conversion and maleic anhydride selectivity are considerably increased when NbPO is associated to VPO.

The physicochemical examination of the VPO–NbPO catalysts reveals the presence of the only crystallised $(VO)_2P_2O_7$ phase with a higher relative intensity of the (024) line as compared to the (200) one, which is typical of a VPO catalyst prepared from $VOHPO_4$, $0.5H_2O$ following the VPD route [12]. This is confirmed from the ^{31}P SEM NMR study. It is illustrated in Fig. 7 for the $VPO_{(3.2)}$–$NbPO_{(1)}$ activated catalyst. The ^{31}P SEM NMR signal at −18.0 ppm which should normally be attributed to NbPO in $(VO)_2P_2O_7$–NbPO catalyst is observed 10 ppm lower than the pure NbPO material (−8 ppm, see Fig. 4a). This is indicative of a modification of the P environment in NbPO, due, probably to a doping of V.

4. Discussion

The improvement of the catalytic performances observed for the mild oxidation of *n*-butane justifies a large interest in the modification of VPO by NbPO. The question which emerges from these results is: how does NbPO influences the catalytic properties of the VPO system. Is there a doping effect on VPO or a synergetic effect induced by Nb? From this study it appears that there is an influence of Nb on the morphology of the $VOHPO_4$, $0.5H_2O$ precursor and on the morphology of the final activated $(VO)_2P_2O_7$ catalyst: this is obvious from the relative intensity of the XRD lines of the VPO precursor and of the $(VO_2P_2O_7$ catalyst favouring a VPD type route morphology [12]. The ^{31}P NMR (MAS and spin echo mapping) and the EDX-STEM studies bring other interesting informations: the ^{31}P NMR spectra by spin echo mapping of the VPO–NbPO precursors show two signals at about −10 ppm, and at 1710/1750 ppm which are respectively characteristic of NbPO and of the $VOHPO_4$, $0.5H_2O$ precursor [14]. The higher value of the signal of $VOHPO_4$, $0.5H_2O$ (1730–1740 ppm instead of 1625 ppm normally observed for this VPO precursor [14]) shows, in this material, a modification of the environment of P, due, probably, to the presence of Nb at show distance which should be indicative of a doping effect. The hypothesis of Nb-doping is also supported by EDX-STEM which shows that Nb is always observed on the isolated $VOHPO_4$, $0.5H_2O$ platelets which have the typical sand-roses morphology of the VPO precursor. The ^{31}P MAS-NMR spectra of the VPO–NbPO precursors show two signals near 0 and −10 ppm, characteristic of the ^{31}P–O–^{51}V and ^{31}P–O–^{93}Nb moieties, respectively. Indeed in NbPO,

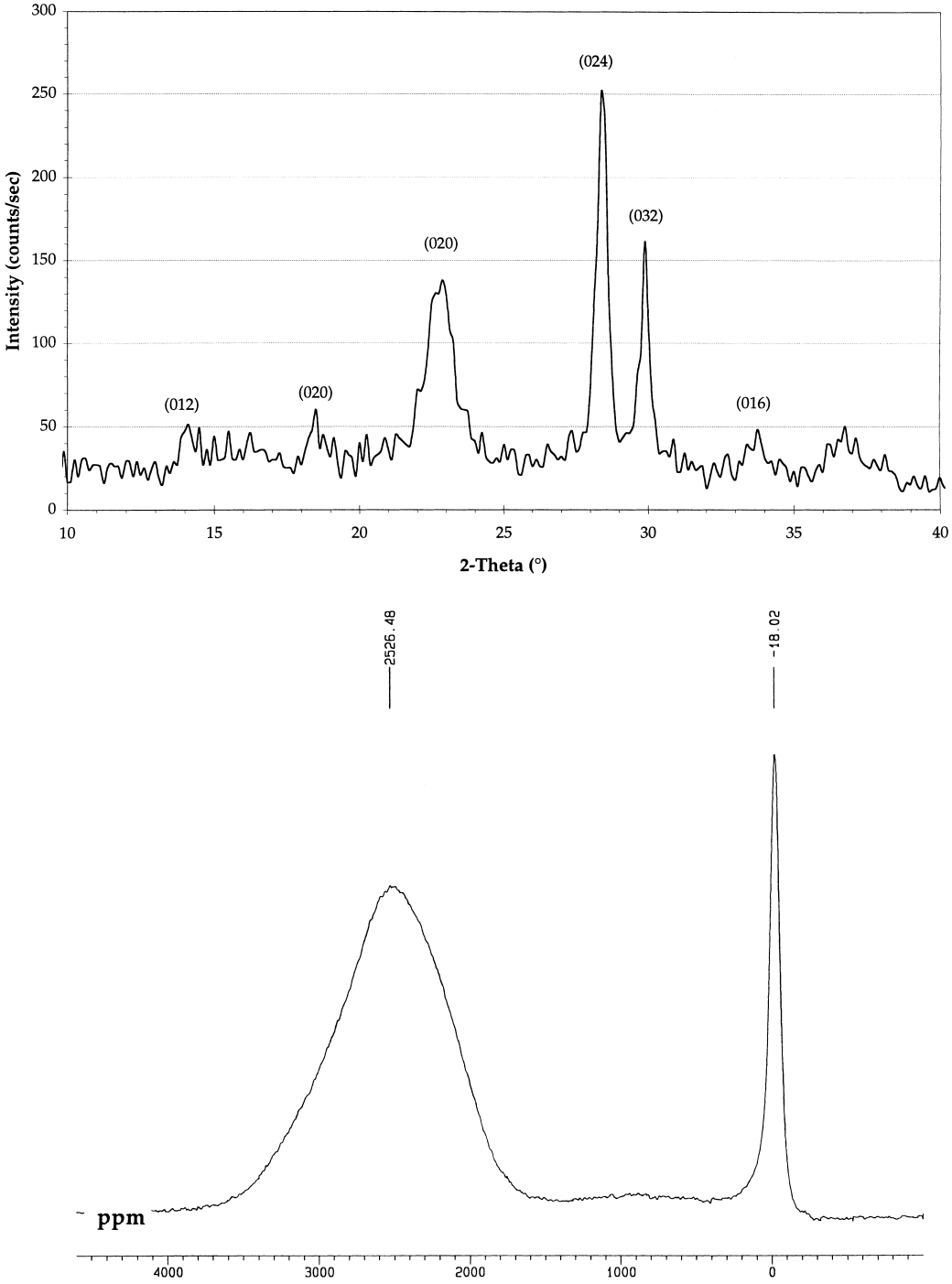

Fig. 7. XRD and ^{31}P SEM NMR spectrum of the activated $VPO_{(3.2)}$–$NbPO_{(1)}$ catalyst.

only the second signal is observed (at −8 ppm). The relative intensity of these two signals (Fig. 4b) changes with an increase of the signal near 0 ppm as compared to the signal at −8, −10 ppm at low NbPO content. It is proposed that Nb should influence the V^{4+}/V^{5+} redox in VPO following the corresponding equilibrium:

$$Nb^{5+} + V^{4+} \rightarrow Nb^{4+} + V^{5+}$$

Indeed NbPO appears to be an amorphous Nb^{5+} material derived from a $NbOPO_4$ phase (the XRD spectrum of NbPO shows contributions at the same position of the main lines of $NbOPO_4$ obtained by calcination at 900°C of the amorphous NbPO material). This hypothesis which should explain the improvement of the VPO catalytic performances by Nb and the speeding up of the activation time has to be confirmed by an XPS analysis of the VPO–NbPO precursor and of the corresponding VPO–NbPO catalyst.

5. Conclusions

The addition of NbPO material used in this study improves the catalytic performances of the VPO catalysts for *n*-butane oxidation to maleic anhydride. This effect is evidenced at low VPO/NbPO ratio. Another interesting feature of the addition of this material is a strong improvement of the activation time of the VPO precursor which will be important for industrial applications. The addition of Nb to VPO catalysts will be also interesting to improve the mechanical strength of the VPO pellets to be used in fixed bed reactors. A modification of the morphology of the VPO precursor, when it is associated with NbPO, has been evidenced by XRD, by TGA-DTA (from the conditions of transformation of the VPO–NbPO precursor) and it has been confirmed by SEM (from the different VPO morphologies observed). By ^{31}P NMR spin echo mapping, there are evidences for a doping effect of Nb on the VPO matrix. It is suggested that Nb influences the V^{5+}/V^{4+} ratio both at the level of the $VOHPO_4$, $0.5H_2O$ precursor and of the $(VO)_2P_2O_7$ catalyst. This does not exclude any synergetic effect between VPO and NbPO but this has to be studied using a well defined NbPO material. The catalytic improvement observed is an highly important result since it is well known that any improvement of the vanadium phosphorus oxides catalysts should go through a better control of the superficial V^{5+}/V^{4+} ratio on the final $(VO)_2P_2O_7$ matrix [6].

References

[1] B.K. Hodnett, Catal. Rev. Sci. Eng. 27 (1986) 373.
[2] B.K. Hodnett, Catal. Today 1 (1987) 477.
[3] G. Centi, F. Trifiro, J.R. Ebner, J.M. Francheti, Chem. Rev. 88 (1988) 55.
[4] J.C.Volta, K. Bere, Y.J. Zhang, R. Olier, in: S.T. Oyama, J.W. Hightower (Eds.), Catalytic Selective Oxidation, ACS Symposium Series, Vol. 523, 1993, p. 217.
[5] M. Abon, K.E. Bere, A. Tuel, P. Delichère, J. Catal. 156 (1995) 28.
[6] K. Aït-Lachgar, M. Abon, J.C. Volta, J. Catal. 171 (1997) 383.
[7] G.J. Hutchings, Appl. Catal. 72 (1991) 1.
[8] R.A. Overbeek, A.R.C.J. Pekelharing, A.J. Van Dillen, J.W. Geus, Appl. Catal. 135 (1996) 231.
[9] J.M. Bueno, G.K. Bethke, M.C. Kung, H.H. Kung, 9° Congresso Brasileiro de Catalise, Sao Paulo, 1997.
[10] I. Matsuura, T. Ishimura, S. Hayakawa, N. Kimura, in Abstract, Second International Symposium on Niobium Compounds, in abstracts, Tokyo, 1995, p. 39.
[11] I. Matsuura, T. Ishimura, S. Hayakawa, N. Kimura, Catal. Today 28 (1996) 133.
[12] M.T. Sananés-Schulz, F. Ben Abdelouahab, G.J. Hutchings, J.C. Volta, J. Catal. 163 (1996) 346.
[13] V. Martin, J.M. Millet, J.C. Volta, J. Thermal Anal. 53 (1998) 111.
[14] M.T. Sananés, A. Tuel, G.J. Hutchings, J.C. Volta, J. Catal. 148 (1994) 395.